

**PHYSIOLOGICAL CHANGES LEADING TO OBESITY IN ACTIVE 13-LINED
GROUND SQUIRRELS (*ICTIDOMYS TRIDECEMPLINEATUS*)**

By

Michelle M. Sonsalla

Obesity is a significant health issue in the developed world. During the pathogenesis of obesity, drastic changes in the gut microbiota lead to intestinal inflammation and increased intestinal permeability, resulting in chronic, low-grade inflammation in white adipose tissue that leads to fattening and insulin resistance. 13-lined ground squirrels (*Ictidomys tridecemlineatus*) naturally fatten in preparation for hibernation and thus we propose that they may be a good model for weight gain in humans. We studied 13-lined ground squirrels during their active season and monitored calorie consumption, body mass, glucose tolerance, adipose mass, and adipose inflammation. Calorie consumption peaked nine weeks after emergence then decreased, whereas body mass continued to increase until weeks 13-15 before it leveled off. Glucose tolerance was relatively constant for most of the active season, with a spike in glucose intolerance 18 weeks post-emergence before returning to similar levels as before. Adipose samples from squirrels were collected throughout the active season and analyzed using qRT-PCR and ELISA to determine changes in immune state. Adipose tissue exhibited significant shifts in immune cell and cytokine levels during the development of obesity. These results suggest that changes in weight gain continue after food intake decreases and adipose immune state during the development of obesity in 13-lined ground squirrels follow the same progression as in other animal models, displaying levels of chronic, low-grade inflammation during obesity.

PHYSIOLOGICAL CHANGES LEADING TO OBESITY IN ACTIVE 13-LINED
GROUND SQUIRRELS (*ICTIDOMYS TRIDECIMLINEATUS*)

by

Michelle M. Sonsalla

A Thesis Submitted
In Partial Fulfillment of the Requirements
For the Degree of

Master of Science

Biology

at

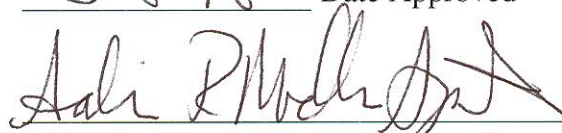
The University of Wisconsin Oshkosh
Oshkosh WI 54901-8621

May 2018

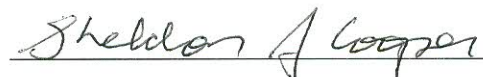
COMMITTEE APPROVAL



Date Approved



Date Approved



Date Approved

PROVOST AND
VICE CHANCELLOR



Date Approved

FORMAT APPROVAL



Date Approved

ACKNOWLEDGEMENTS

I would like to thank Laurana Rudenas, Santidra Love, Margot Elliot, Hannah Follett, and Kelli Trester (University of Wisconsin Oshkosh) for the large amount of assistance they provided with animal husbandry and tissue collection; and Dr. Dana Merriman, Dr. Colleen McDermott, and Sara Hagedorn (University of Wisconsin Oshkosh) for their expertise in the care of the study animals. I would also like to thank my committee members, Dr. Sheldon Cooper, Dr. Sabrina Mueller-Spitz, and advisor Dr. Courtney Kurtz for their unwavering guidance during my graduate research. The author gratefully acknowledges the support of the UW Oshkosh Faculty Development Grant program and the UW Oshkosh Office of Student Research and Creative Activity (OSRCA; Student-Faculty Collaborative Grant to Sonsalla) for funding this project.

TABLE OF CONTENTS

	Page
LIST OF TABLES.....	iv
LIST OF FIGURES.....	v
CHAPTER I: INTRODUCTION.....	1
Obesity.....	1
Pathogenesis of Obesity.....	5
Gut Microbiota Dysbiosis.....	5
Intestinal Inflammation.....	7
Adipose Inflammation.....	8
Animal Models of Obesity.....	11
CHAPTER II: BODY.....	15
Introduction.....	15
Materials and Methods.....	17
Results.....	24
Discussion.....	32
CHAPTER III: CONCLUSION.....	40
REFERENCES.....	42

LIST OF TABLES

		Page
Table 1.	Calendar dates corresponding to GTT and tissue collection weeks.	19
Table 2.	Primers and annealing temperatures used for WAT qPCR.....	22
Table 3.	Body Temperature and Adipose Mass at Tissue Collection.....	27

LIST OF FIGURES

		Pages
Figure 1.	Overview of the pathogenesis of obesity.....	11
Figure 2.	Changes in body mass and caloric intake during the active season..	25
Figure 3.	Glucose tolerance measured throughout the active season.....	26
Figure 4.	Expression of immune markers in iaWAT and mWAT.	30
Figure 5.	Levels of IL-10 and TNF α protein in iaWAT and ingWAT.....	31

Chapter I

Introduction

Obesity

Prevailing attitudes have long held that to maintain a constant weight, energy intake must equal energy expenditure. Thus, any disturbance in this “energy balance” will result in changes to body mass and, should intake exceed expenditure, obesity occurs. Research in humans has shown that the cause of obesity is not this simple (1). Energy homeostasis is maintained through complex communication between the gastrointestinal (GI), nervous, endocrine and immune systems. In order to adequately maintain energy homeostasis, the brain, particularly the hypothalamus, needs accurate information about the body’s current stored energy and ongoing nutrient intake. These signals (i.e. hormones and cytokines) can be relayed to the brain by molecules crossing the blood brain barrier (BBB) or via stimulation of afferent vagal nerves.

Some of these signals regulate the start and end of meals. Meal initiation is determined by a variety of factors, including time of day, social factors and levels of different hormonal factors, such as ghrelin. Ghrelin, a peptide secreted primarily by the stomach and intestine, acts to stimulate hunger and food intake (2–4). When circulating levels of ghrelin are high, appetite is increased. As food is consumed, plasma ghrelin levels decrease along with appetite (2–4). Satiety is triggered by gastric and intestinal distension and nutrient arrival in the small intestine, which leads to the release of the hormones peptide YY (PYY) and cholecystokinin (CCK) (3, 4).

Another important group of signals are those that relay information regarding current stored energy levels, such as leptin and other adipokines. Adipokines are signaling molecules secreted by adipose tissue. Leptin is a hormone secreted by adipose tissue in relation to the amount of fat stored. Increased leptin signaling in times of high fat mass acts on both the central nervous system and peripheral tissues to induce satiety and increase whole body glucose utilization (2, 4–7). In the central nervous system, leptin binds receptors in the hypothalamus and leads to activation of the sympathetic nervous system, which promotes glucose mobilization (2, 5–7). This works via signal transducer and activator of transcription (STAT) proteins, which regulate the expression of orexigenic or anorexigenic genes (6, 7). Leptin also acts directly on adipocytes through paracrine and autocrine signaling to alter expression of genes involved in lipid metabolism (7).

Finally, hormones involved in regulating glucose homeostasis also play an important role in controlling energy metabolism. Insulin is one of the main anabolic hormones in the body. Insulin is secreted by the β cells found in the pancreatic Islets of Langerhans (2). When food is consumed and absorbed, a rise in blood glucose triggers the release of insulin from the pancreas (2). Insulin promotes glucose uptake by cells as well as storage of glucose as glycogen and conversion to triglycerides for storage in adipose tissue. Thus, when insulin rises, blood glucose levels decrease (2, 7). Another important hormone, glucagon, works opposite insulin. Glucagon is secreted by the α cells in the Islets of Langerhans and leads to the breakdown of storage forms and the release of glucose into the blood (2). Contrary to insulin, glucagon is released in response to low

blood glucose levels, such as what occurs between meals. Glucagon and insulin inhibit each other's actions and, along with other factors (catecholamines, cortisol, growth hormone, insulin-like growth hormone and thyroid hormone), maintain blood glucose levels within a narrow range of tolerance (2). During obesity, insulin resistance may develop, during which there is a disruption of insulin-mediated glucose uptake, resulting in elevated blood glucose levels (2, 43, 47-48).

The primary control center in metabolism and appetite is the central nervous system, particularly the hypothalamus. The hypothalamus responds to signals from the periphery, such as leptin and insulin, by activating sympathetic and parasympathetic nerves (6). As part of their function, the sympathetic and parasympathetic nervous networks (part of the autonomic nervous system) work to regulate glucose and fat metabolism to maintain homeostasis by innervating important metabolic tissues of the body, including the liver, pancreas, adipose tissue and muscles (6). Through regulation of sympathetic and parasympathetic outflow, the brain is able to regulate whole body energy homeostasis.

The high prevalence of obesity in today's society may be due to a number of different factors, including the high-fat, high-sugar, and highly palatable modern diet, sedentary lifestyles, and genetic contributions (1, 8–10). The modern diet is composed primarily of processed foods and consists of high levels of both fats and carbohydrates, which increases the amount of calories consumed even when a relatively normal meal size is consumed (1, 11). In addition, normal feeding behavior is altered by the introduction of liquid sugar consumption (such as in soda), which has been found to

increase the number of meals consumed, without a corresponding decrease in meal size (1, 8). This leads to an overall increase in food intake. On the other side of the energy balance, modern society encourages less physical activity through accessibility of automotive transport, reduced physical demands at work, and prevalence of internet and television in homes (12). Finally, human evolution has contributed to the development of a metabolically “thrifty” genotype (9). Our metabolism leans toward the storage of energy during food abundance so that survival is increased when food is scarce. This was beneficial when food availability was uncertain but in today’s developed countries, when excessive amounts of food are readily available, particularly for affluent individuals, these “thrifty” genes are maladaptive and contribute to the prevalence of obesity. This increase in energy intake with the associated decrease in energy expenditure along with the interactions of metabolically “thrifty” genes leads to a significant accumulation of energy storage in the form of fat.

Obesity in humans is defined as a body mass index (BMI; weight in kilograms divided by height in meters) of greater than 30 kg/m^2 (12). In general, obesity is a chronic disease characterized by the accumulation of excess fat stored in adipose tissue and other organs (10, 13). Today, obesity is an epidemic in the United States and is becoming more prevalent around the world. According to a 2016 World Health Organization report, 1.9 billion adults were overweight and of these more than 650 million were considered to be obese (14). In addition to the health problems associated with obesity itself, such as insulin resistance, high blood pressure, and breathing problems, there are a number of

comorbidities linked to obesity, including type II diabetes, cardiovascular disease, and some cancers (11–13, 15).

Pathogenesis of Obesity

Gut microbiota dysbiosis.

The gut microbiota is composed of thousands of microbes (16–27). The majority of the microbiota is bacteria, with most belonging to the phyla *Bacteroidetes* and *Firmicutes*, but is also composed of some eukaryotes, archaea, and viruses (16–27). The gut microbiota serve the host by aiding in digestion through production of additional digestive enzymes not produced by the human body as well as development of the immune system (16, 21, 22, 24–27). During gestation and at birth, the mother’s microbiota contributes greatly to the composition of an individual’s microbiota (24, 26). The microbiota community continues to develop throughout childhood. Once an “adult-like” microbiota has developed, the community remains relatively constant, with long-term dietary habits and genetics playing important roles in microbiota composition (26, 27). Despite the relative consistency of the adult microbiota, changes in diet can rapidly induce small changes in the microbiota composition, particularly diets high in fat and carbohydrates, like the so-called Western diet (19, 20, 22–27).

The gut microbiota is implicated in the development of obesity. Obesity is typically characterized by an increase in the ratio of *Firmicutes* to *Bacteroidetes*, as well as an overall decrease in bacterial diversity (19–27). *Firmicutes*, such as *Clostridium*, *Lactobacillus*, *Methanobrevibacter smithii*, and *Ruminococcus spp.*, have a greater

fermentation efficiency than *Bacteroidetes* (24, 26). Fermentation by the gut microbiota is the breakdown of dietary fibers into short chain fatty acids (SCFAs), which can be absorbed and utilized by the host (24, 26). Increased SCFA production leads to an increase in calories absorbed by the host and thus less caloric waste from the food. This allows the host to absorb more energy even if food ingestion is decreased. A simple increase in energy intake is not the only way that microbiota dysbiosis contributes to obesity and metabolic disease. The gut microbiota has been found to regulate the secretion of fast-induced adipocyte factor, which inhibits lipoprotein lipase, leading to decreased free fatty acid storage in the liver or muscles and increased lipid storage in white adipose tissue (WAT) (24, 26). The shift in the gut microbiota leads to an increase in endotoxin (e.g., lipopolysaccharides [LPS]) production, which enter the bloodstream and travel to distant tissues, where immune cell activation leads to an increase in systemic inflammation (16–27). Certain microbial groups have well-documented effects on host metabolism and immunity. Segmented filamentous bacteria (SFB) regulate the pro-inflammatory Th17 response and have been found to decrease during obesity (23, 25). *Akkermansia muciniphila*, a member of the phylum *Verrucomicrobia*, utilizes intestinal mucins as its sole energy source (25, 26). *A. muciniphila* lives within the mucus layer and acts to improve intestinal barrier function, which results in decreased plasma endotoxin levels and subsequent adipose inflammation and obesity. It is no surprise that *A. muciniphila* abundance is inversely correlated with obesity (25). Overall, high fat diets and obesity are associated with a dysbiosis of the gut microbiota, leading to shifts in energy intake and storage.

Intestinal inflammation.

Changes in the GI microbiota can lead to changes in the intestinal immune system. The intestinal barrier, an important part of innate immunity, separates the gut microbiota from host tissues and controls the contact between the two while regulating the uptake of nutrients and water (16, 18, 28–30). The intestinal barrier is made up of a thick layer of mucus, which is composed of both mucin and antimicrobial compounds, and a single layer of epithelial cells (16, 18, 28). The permeability of the intestinal epithelium is determined by the tight junctions between cells. Interactions between altered gut microbiota and host epithelial cells can lead to increased permeability which allows the translocation of endotoxins. The presence of endotoxins in the underlying tissue activates immune cells and drives the secretion of pro-inflammatory cytokines that further increase gut permeability (29, 30).

These endotoxins activate immune cells by binding to so-called pattern recognition receptors (PRRs). These receptors, such as Toll-like receptor 4 (TLR4), are found on intestinal epithelial cells and various immune cells such as monocytes, macrophages, and dendritic cells. Binding of an endotoxin or other ligand to a PRR results in the activation of the transcription factor nuclear factor kappa-light-chain-enhancer of activated B cells (NF- κ B) (19, 20, 22, 31). NF- κ B promotes expression of pro-inflammatory cytokines, like tumor necrosis factor (TNF) α , interleukin (IL)-1 β , IL-6 and monocyte chemoattractant protein (MCP)-1. TNF α can increase intestinal permeability by weakening tight junctions and inducing high levels of epithelial cell shedding as well as increasing the ability of immune cells to migrate into the

inflammatory tissue (28, 29, 32, 33). IL-6 regulates the differentiation of macrophages, T cells, B cells and other immune cells (34). MCP-1 attracts circulating monocytes into the tissue, where they differentiate into macrophages and secrete more pro-inflammatory cytokines, such as IL-1 β , IL-6, and IL-8 (23, 33). These culminate in an increased in GI inflammation during obesity, particularly in the distal small intestine and proximal colon.

High fat diet and obesity are correlated with the upregulation of antigen-presenting and co-stimulatory factors such as major histocompatibility complex class II (MHC II, specifically HLA-DR), cytotoxic T-lymphocyte associated protein 4 (CTLA4), CD28 and CD80, and inducible T-cell co-stimulator (ICOS), which contribute to the inflammation in GI tissue (35). Diet-associated intestinal inflammation leads to increased numbers of pro-inflammatory immune cells, including Th1 cells, M1 macrophages, dendritic cells, neutrophils and B cells (17, 19, 23, 35–37). On the other hand, populations of anti-inflammatory immune cells, such as regulatory T cells (Treg), Th2 cells, M2 macrophages and type 2 innate lymphoid cells (ILC2), decrease (17, 23, 38). The role of intestinal Th17 cells is more difficult to understand in obesity, as it seems to vary from study to study with no real consensus (17, 18, 39). This so-called “sub-clinical” intestinal inflammation that occurs in response to changes in gut microbiota can lead to the development of inflammation in metabolic tissues, insulin resistance (IR) and obesity (17, 19, 23, 35–37).

Adipose inflammation.

White adipose tissue (WAT) is involved in energy metabolism, food intake, insulin sensitivity and immunity through the release of adipokines, which signal the

endocrine, immune and nervous systems (40, 41). During obesity, the release of adipokines is altered dramatically. Increased secretion of pro-inflammatory molecules from WAT, such as leptin, TNF- α , IL-6 and MCP-1, contribute to the chronic, low grade inflammation present during obesity (40, 41). Lean WAT is composed of adipocytes, pre-adipocytes, endothelial cells and immune cells (40). There are a variety of immune cells present in WAT, including macrophages, mast cells and T cells. In lean WAT, the population of immune cells is low. For example, macrophages only comprise 5% of the cells in lean WAT and are scattered throughout the tissue (40). The majority of these macrophages are M2, or “alternatively activated”, macrophages that are characterized by anti-inflammatory cytokine production (42). M2 macrophages are important for the promotion of tissue repair, prevention of inflammatory responses and maintenance of proper adipocyte function and insulin sensitivity (42). The majority of T cells in lean WAT are Treg and Th2 cells, which are generally anti-inflammatory in nature. These T cells act to promote the differentiation of M2 macrophages and the sensitivity of cells to insulin (43). Adipocytes in lean WAT contribute to this anti-inflammatory state through increased secretion of anti-inflammatory adipokines, such as adiponectin, and decreased secretion of pro-inflammatory adipokines, such as leptin.

During obesity, there is an increase in adipose tissue mass, without a corresponding increase in blood flow to the tissue, resulting in hypoxia and higher levels of adipocyte death (40). Increases in hypoxia-related gene expression and the number of dead cells result in increased pro-inflammatory cytokine (i.e., leptin, TNF- α , IL-6, and MCP-1) production by adipocytes (40, 41, 44). Macrophages are found in obese WAT at

much higher numbers than in lean WAT, making up as much as 50% of total WAT cells (40). The rapid increase in adipose tissue macrophages is due primarily to an influx of bone marrow-derived monocytes, caused by an increase in secretion of MCP-1.(44). Obese WAT macrophages tend to be more of the M1, or “classically activated”, phenotype, which is characterized by pro-inflammatory cytokine production and increased generation of reactive oxygen species (ROS) (40, 42). Obese WAT is also characterized by distinct changes in T cell populations. WAT secretes chemokines which recruit T cells to adipose tissue early in obesity (45). Like the macrophages, there is an overall increase in T cell numbers as well as a major shift in the types of T cells compared to lean WAT. The number of Treg cells decreases early in the development of obesity due to changes in adipokine secretion (46). Treg cells function to repress the proliferation of pro-inflammatory Th1 cells, so a decrease in Treg cell populations is accompanied by a shift from Th2 to Th1 cells. This shift is significant because Th1 cells secrete pro-inflammatory cytokines, while Th2 secrete mainly anti-inflammatory cytokines (43, 45, 47). The loss of Treg and Th2 cells in WAT during obesity also contributes greatly to the development of IR, as both have insulin-sensitizing effects (43, 47). However, it has been recently proposed that IR, instead of being caused by adipose inflammation, may actually contribute to the development of adipose inflammation (48). Regardless of which comes first, obesity is often characterized by both adipose inflammation and IR. Thus, changes in the immune milieu of WAT during obesity correspond with adipose inflammation and IR.

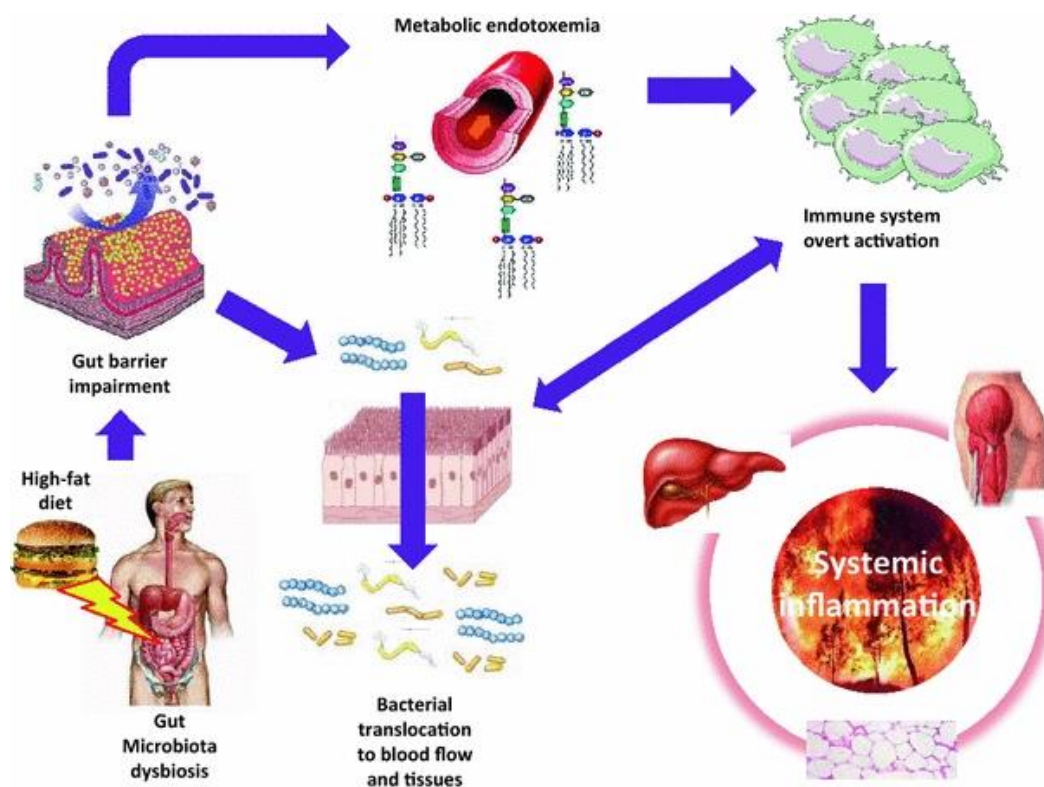


Figure 1.

The development of obesity begins with a dysbiosis of the gut microbiota due to changes in diet, particularly high-fat and high-sugar diets. This leads to increased gut permeability, which allows endotoxins to enter the bloodstream and travel to metabolic tissues, where immune system activation results in systemic inflammation. (Figure from Burcelin et al. 2011) (49)

Animal Models of Obesity

Due to the high prevalence of obesity and the significant health risks that it imposes, there is a dire need for more research in order to understand the pathology of disease and develop pharmaceutical treatments. Most obesity research involves animal models. Animal models may be monogenic (i.e., obesity induced due to a single gene mutation, often in the leptin signaling pathway) or polygenic (i.e., obesity induced due to a variety of genetic variations and environmental factors) (10–12, 50). Monogenic

models typically include mouse and rat models, such as the *ob/ob* mouse or Zucker Fatty Rat (11). These models are important for pharmaceutical applications where there is a need for a clear phenotype that can be monitored for alterations (11). Polygenic models include rodents as well as non-human primates and pigs (10–13, 50). These models are important because there are very few instances of human obesity arising from a single genetic mutation. Instead, most occur as the result of many genes each carrying a small risk on its own (50). Obesity in polygenic models is typically induced by decreased energy expenditure or increased caloric intake via a Western or cafeteria diet (a varied and palatable high fat, high carbohydrate diet that promotes hyperphagia) or commercial high fat, high carbohydrate pellet diet (10, 11, 50). Finally, some studies have used seasonal models of obesity, such as Siberian and Syrian hamsters. In these models, changes in body weight and adiposity vary in a yearly cycle, triggered by photoperiod (10, 50).

The unique nature of the latter models is that these hamster species can use hibernation or torpor. Mammals tend to keep a relatively constant body temperature (T_b) of 36–38°C, but this can be very costly during winter, when ambient temperatures (T_a) are low (51, 52). For some, especially small rodents, maintaining a constant T_b during the winter can be difficult, particularly when food is scarce. To combat this, some mammals have adopted a strategy of hibernating for 7–9 months of the year, during which time metabolic processes and T_b decrease dramatically (51–54). This gives them an energy savings of 85–88% compared to the estimated energy needed to maintain a T_b of 37°C in the cold (51, 52). Hibernation is a prolonged period of fasting and inactivity in which the

majority of energy is supplied by endogenous reserves, particularly triglycerides stored in WAT. By the end of the hibernation season, up to 50% of the animal's body mass has been lost and this must be regained in the short 3-5 months before the subsequent hibernation period (51, 53–55). The short active season is characterized by hyperphagia, a doubling or even tripling of food intake and increase in body mass by up to 50% (mainly in the form of WAT, resulting in an increase in percent body fat). During this time, the preferred diet shifts particularly to seeds and other foods high in polyunsaturated fats (51, 54). As peak body mass is reached, IR develops but is quickly reversed as the animals begin enter hibernation (54). At the same time, metabolic rate and food intake decrease and energy balance shifts toward rapid weight gain, largely due to restructuring of the gut microbiota into a community more efficient at harvesting and storing energy (52, 55). Surprisingly, there is not a decrease in resting metabolic rate or activity levels in hibernators during the period of weight gain, but rather energy sparing techniques are used to maintain the optimal body mass until the animals enter hibernation (56). The animals then enter hibernation, which is characterized by long bouts of torpor interrupted periodically by short arousals to euthermia (6-24 hours long) (51, 52).

Hibernators are unique and valuable models of obesity because they represent a natural example of rapid WAT mass gain. Each year, they undergo a cycle of rapid weight gain and loss, during which they develop obesity and IR. Unlike polygenic models, hibernators are able to develop obesity without the use of a high-fat diet and are even able to gain similar amounts of body mass during the active season when on a low fat or calorie-restricted diet (55). Also, hibernators could be valuable models for

pharmaceutical treatments. These animals are so genetically programmed to fatten, that if a treatment is able to offset the development of obesity in them, there is a strong possibility that it should work for other animal models and humans.

Chapter II

Body

Introduction

Obesity is a serious epidemic in the United States, as well as in the rest of the world. According to a 2016 report by the World Health Organization, 650 million adults were considered obese (14). In addition to health risks due to obesity itself, a number of comorbidities are associated with obesity, including type II diabetes, cardiovascular disease and some types of cancers.

The pathogenesis of obesity is still not well known. It is thought to begin with diet-induced changes in gut microbiota composition and low-grade intestinal inflammation, followed by subclinical inflammation in adipose tissue and insulin resistance (IR) (13, 15, 57). Dysbiosis of the microbiota leads to intestinal inflammation and increased intestinal barrier permeability, as well as increased energy harvest from ingested nutrients (23). Increased permeability facilitates the translocation of bacterial products, such as lipopolysaccharides (LPS), across the intestinal barrier into the blood, resulting in low-grade inflammation of metabolic tissues, which are adipose tissue, muscle, and the liver (so called “metabolic inflammation”) (23). Adipose tissue produces abnormal amounts of adipokines, including elevated levels of leptin and reduced levels of adiponectin. This, along with the production of pro-inflammatory cytokines, like tumor necrosis factor (TNF)- α , lead to metabolic inflammation which can cause IR via interactions between cytokine and insulin signaling pathways (15). Both IR and the

increased efficiency of energy harvest from food by gut microbes contribute to an increase in lipid storage in white adipose tissue (WAT).

Due to the high prevalence of obesity and the serious health risks associated with it, there is a need for research on both the pathogenesis of obesity and pharmaceutical treatments. Much of this research involves animal models, which are typically monogenic (obesity induced due to a single gene mutation), polygenic (obesity occurs due to the interactions of a number of genes with a high fat diet) or seasonal (adipose mass loss and gain occur in a yearly cycle) models (10–12, 50). The benefit of seasonal models is that the increased adiposity occurs independently of a western high fat diet (HFD). This allows accurate assessment of changes in the physiology associated with obesity independent of changes due to HFD ingestion. Hibernators are one example of a seasonal model, in which body mass and adiposity rapidly increase during the short active season and decrease during the long hibernation period (51, 53–55, 58–60). Because hibernation is characterized by prolonged fasting, it is important that hibernators accumulate sufficient energy stores to last them until the following active season. In this study, we used a hibernator, the 13-lined ground squirrel (*Ictidomys tridecemlineatus*), to define a timeline of events that lead to increased adiposity during the active season. We hypothesized that there would be a rapid increase in body mass and adiposity during the active season, but that caloric intake would peak before the maximum body mass was achieved. We also hypothesized that white adipose tissue (WAT) would progress to a more inflammatory state throughout the active season, as shown by increased pro-inflammatory cytokines and decreased anti-inflammatory cytokines. Finally, we

hypothesized that glucose intolerance and insulin resistance would reach a peak late in the active season, then would drop off as the squirrels begin to show signs of hibernation, as shown in other hibernating species (54).

Materials and Methods

Animals.

Yearling female 13-lined ground squirrels (n=30) were obtained from the UW Oshkosh squirrel colony and allowed to hibernate. On April 14, 2017, when interbout arousals were becoming more frequent for the majority of animals, the ground squirrels were removed from the hibernaculum and housed individually in standard rat cages (10" wide x 19" long x 8" tall) with unlimited access to water at ~20°C. Light-dark cycles were adjusted as follows during the active season: 12.5 hours of light/11.5 hours of dark April 14, 2017-June 5, 2017, 15.5 hours light/8.5 hours dark June 6, 2017- August 8, 2017, 14 hours light/10 hours dark August 9, 2017-August 20, 2017, 13.75 hours light/10.25 hours dark August 21, 2017-September 3, 2017, and 13.25 hours light/10.75 hours dark September 4, 2017-September 8, 2017. All procedures involving animals were approved by the UW Oshkosh Institutional Animal Care and Use Committee (Protocol #0026-000298-11-15-16).

Feeding regimen and weekly weigh-ins.

The squirrels were fed Teklad Global 18% Protein Diet (#2018, Envigo, Madison, WI) ad libitum (food was added throughout the week to ensure that the squirrels would not run out at any point) and supplemented with sunflower seeds (6.44 g [1 tbsp]) once

per week. The amount of food (in grams) added to the cage each day was measured and the total food added for the week calculated (89.4 ± 5.61 g on average). The amount of food remaining in the cage at the end of each week was recorded and subtracted from total food added to determine the amount of food consumed weekly. These values were then converted to kilocalories consumed based on the nutritional content of the diet. Body mass for each squirrel was recorded weekly. To minimize stress, this was done during weekly cage cleaning where a clean cage was tared on a balance prior to addition of the squirrel.

Glucose tolerance tests.

Intraperitoneal glucose tolerance tests (IPGTT) were performed throughout the active season as an indicator of glucose intolerance and IR (Timing of GTTs shown in Table 1). A subset of six squirrels was used each time. Before the GTT, the squirrels were fasted for 5 hours by moving them to a clean cage with bedding and ad libitum water but no food. Anesthesia was induced in a 3-liter induction chamber using 5% isoflurane. After an appropriate plane of anesthesia was reached, the squirrel was transferred to dorsal recumbancy on a heating pad or heated rice sacks and 3-5% isoflurane was delivered via nose cone. The ventral side of the tail was shaved and cleaned with ethanol. A 22-G needle was used to collect a drop of blood from the tail artery for glucose measurement using a Contour Next glucometer (manufacturer calibrated). Gauze was used to stop the bleeding. The squirrel was then injected intraperitoneally with 1 g/kg D-glucose in sterile saline. Additional drops of blood were collected and analyzed with the glucometer at 15, 30, and 60 minutes post injection. Once

the final blood sample was collected, the animal was removed from anesthesia and allowed to recover in its cage on a heat source. Food was returned once the animal had fully recovered from anesthesia. Glucose tolerance test results were analyzed by plotting time after injection against blood glucose levels and using a self-made excel program to calculate the area under the curve (AUC). A small AUC corresponds to high glucose tolerance, whereas a large AUC corresponds to low glucose tolerance, and potentially IR.

Table 1.

Calendar dates corresponding to GTT and tissue collection weeks.

Calendar date	Weeks after emergence	Event
April 14, 2017	0	Removed from hibernaculum
April 21, 2017	1	GTT
May 19, 2017	5	GTT
June 21, 2017	10	GTT
June 28, 2017	11	Tissue Collection
July 21, 2017	14	GTT
July 26, 2017	15	Tissue Collection
August 2, 2017	16	GTT
August 9, 2017	17	Tissue Collection
August 16, 2017	18	GTT
August 23, 2017	19	Tissue Collection
August 31, 2017	20	GTT
September 6, 2017	21	Tissue Collection

Tissue collection.

Squirrels were euthanized throughout the active season (in subsets of 6) for tissue collection. These tissue collections were performed 11, 15, 17, 19, and 21 weeks after emergence (Table 1). Each squirrel was anesthetized in a 2-liter induction chamber using 5% isoflurane, then weighed and euthanized by decapitation. Body temperature was then measured by inserting a small probe into the abdominal cavity through a small incision. Mesenteric (mWAT), retroperitoneal (rWAT), omental (oWAT) and intra-abdominal (iaWAT) visceral WAT depots were removed and weighed. Percent adiposity and obesity were determined based off other rodent models, which stated that obesity was characterized by a percent adiposity of 8.78% or greater (61). Percent adiposity was calculated by summing iaWAT, rWAT, and oWAT then dividing by total body mass and multiplying by 100 (61). A small portion of inguinal adipose tissue (ingWAT, a subcutaneous WAT depot) was removed as well. Small portions of each WAT depot were placed into 300 μ l of RNAlater (Invitrogen, Carlsbad, CA) for later analysis. Another, larger portion was flash frozen in liquid nitrogen and stored. All collected tissues were stored at -80°C until used.

Adipose RNA extraction.

RNA was isolated from iaWAT and mWAT adipose samples that had been stored in RNAlater using a Total RNA Mini Kit (IBI Scientific, Peosta, IA). Approximately 40 mg of WAT was transferred to a clean, nuclease-free 1.5 ml tube, then RB Buffer, β -mercaptoethanol, and two 2.4 mm omni metal beads were added. Parafilm was used to seal the caps and the samples were lysed in a TissueLyzer at a rate of 50 oscillations/s for

5 minutes. The samples were incubated at room temperature for 3 minutes then transferred to a filter column and centrifuged at 1,000 x g for 30 seconds. The filter column was discarded. Ethanol (400 μ l, 70% prepared in nuclease-free water) was added to the filtrate then the ethanol mixture transferred to an RB column. The RB column was centrifuged for 1 minute at 16,000 x g then the flow through was discarded. W1 Buffer (400 μ l) was added to the centrifuge column and centrifuged for 30 seconds at 16,000 x g. The flow through was discarded, 600 μ l of Wash Buffer added to the RB column, then centrifuged for 30 seconds at 16,000 x g. The flow through was discarded, and another 600 μ l of Wash Buffer was added to the RB column. The RB column was centrifuged for 30 seconds at 16,000 x g and the flow through discarded. The RB column matrix was dried by centrifuging for 2 minutes at 16,000 x g. To elute the RNA, the RB column was transferred to a clean, nuclease-free 1.5 ml tube and 50 μ l of nuclease-free water was added to the column. The column was left to stand for at least 1 minute to ensure the water had completely soaked into the matrix, then the column centrifuged for 30 seconds at 16,000 x g. The RB filter was discarded, then the isolated RNA analyzed on a nanodrop spectrophotometer to determine concentration and purity. The isolated RNA was stored at -80°C until further analysis.

Quantitative reverse transcriptase PCR.

cDNA was created from the RNA using an M-MLV Reverse Transcriptase (Promega, Madison, WI). The reaction mixture was set up with 200 ng of RNA using oligo (dt) primers to preferentially target mRNA. The samples were placed in the thermocycler for 5 min at 70°C then immediately placed on ice. A master mix containing

MMLV Reaction Buffer, 2 mM dNTP mix, 25 units Recombinant RNasin Ribonuclease Inhibitor, 200 units M-MLV reverse transcriptase, and nuclease free water was prepared and added to each sample. The samples were incubated in the thermocycler for 60 min at 37°C then stored at -20°C until further analysis. WAT cDNA was analyzed using Bullseye EvaGreen qPCR Mastermix (MidSci, Valley Park, MO) and run on an Applied Biosystems Real Time PCR Machine. The protocol used was as follows: 95°C for 2 min, 40 cycles of 95°C for 15 s, the appropriate annealing temperature (Table 2) for 30 s, and 72°C for 45 s, then 72°C for 2 min, a melt curve of 95°C for 15 s, 60°C for 1 min, and 95°C for 15 s, and a final infinite hold of 20°C. Primers were designed using the annotated 13-lined ground squirrel genome on ensembl.org using the primer3web program. Primer sequences and annealing temperatures used are listed in Table 1.

Table 2.

Primers and annealing temperatures used for WAT qPCR

Gene	Temp	Forward Primer (5' to 3')	Reverse Primer (5' to 3')
Actin	60°C	GGAAATCGTGCGTGACATCA	AGGATTCCATGCCCAGGAAA
FOXP3	62°C	AGGACAGCACCCCTTTTAGCT	AAGACTGCACCACCTCTCTC
MRC1	60°C	TCCTTTCCATGGTCACTGCT	AGAGCCACATCCCTTCAACA
GATA3	60°C	AGATCCAGCACAGAAGGCAG	GGTCTGACAGTTTGCACAGG

ELISA.

iaWAT and ingWAT were analyzed for the levels of specific cytokines. First, approximately 40-70 mg of WAT was measured and placed into a centrifuge tube

containing PBS. The tissue was homogenized by hand with a dounce homogenizer. Enzyme-linked immunosorbent assays (ELISA) were performed for tumor necrosis factor (TNF)- α and interleukins 10 (IL-10) and 6 (IL-6) (both from BD Biosciences, San Diego, CA) following the manufacturer's instructions. A protein assay was performed of the samples in order to normalize cytokine concentrations to total protein. The Pierce BCA Assay Kit (Thermo Fisher Scientific, Waltham, MA) was used following the manufacturer's instructions.

Statistics.

Statistics were run using Minitab statistics program. Normal distribution of the data was assessed with the Anderson-Darling normality test. If data sets were not normally distributed (i.e., body mass, mWAT MRC1 and GATA3, iaWAT GATA3), a log transformation was attempted. If log transformed data was not normally distributed (all cases above), a Kruskal-Wallis test on the non-transformed data was used to determine changes between groups. Mann-Whitney U tests were performed between groups and adjusted with Bonferonni correction. For normally distributed data, one-way ANOVA was used for analyses along with Fisher's LSD post-hoc pairwise comparison. For all tests, p-values ≤ 0.05 were considered significant.

Results

13-lined ground squirrels exhibited significant changes in body mass and caloric intake.

Squirrels were weighed every week beginning at emergence from hibernation on April 14, 2017 until the last set of tissue collections on September 8, 2017. The average body mass at the beginning of the active season was 128.5 g, and then increased significantly ($P < 0.001$) until it reached 226.7 g 20 weeks after emergence, an average mass gain of 98.2 g (Figure 2). Caloric intake increased immediately after emergence, but peaked at nine weeks after emergence before falling to less than initial levels by week 15 ($P < 0.001$, Figure 2). Squirrels were showing signs of torpor by 20 weeks post-emergence with decreased activity and food intake and behaviors consistent with frequent, short “test” torpor bouts (personal observations).

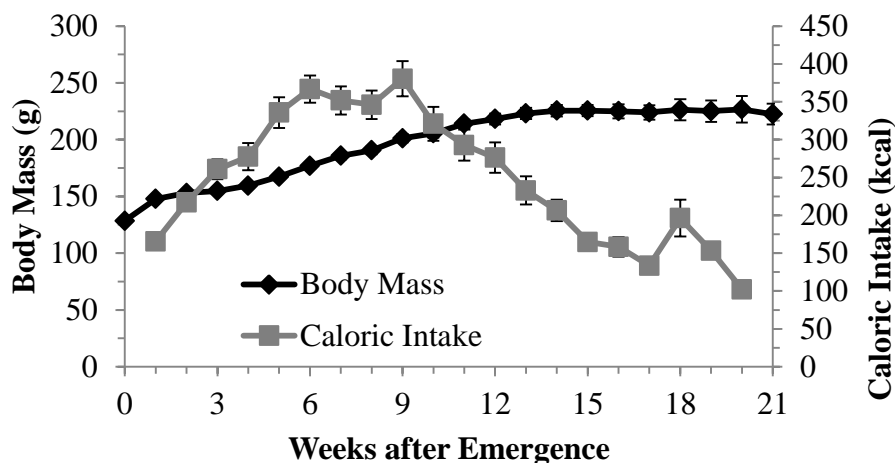


Figure 2.

Changes in body mass (black lines) and caloric intake (gray lines) during the active season. Lines represent mean \pm SE of 3-30 squirrels (later weeks had fewer squirrels because of subsets euthanized for tissue collection). For both body mass and caloric intake, $P < 0.001$.

Glucose intolerance shows a strong trend for a peak at 18 weeks after emergence but is recovered by week 20.

Intra-peritoneal glucose tolerance tests (IPGTT) were used as an indicator of glucose intolerance and IR. The area under the curve (AUC) for IPGTT performed at weeks 1, 5, 10, 14, 16, 18, and 20 on subsets of 6 squirrels was calculated. A larger AUC value signifies more glucose intolerance, due to the blood glucose level remaining at a higher level for longer. The mean AUC for each subset of squirrels was used to determine changes in glucose tolerance over the active season, as squirrels became increasingly obese (Figure 3). There was a trend toward a significant increase in glucose intolerance ($P = 0.077$) at 18 weeks after emergence, but glucose tolerance was recovered by week

20 when the squirrels were showing regular signs of torpor, as has been demonstrated in other hibernators (54).

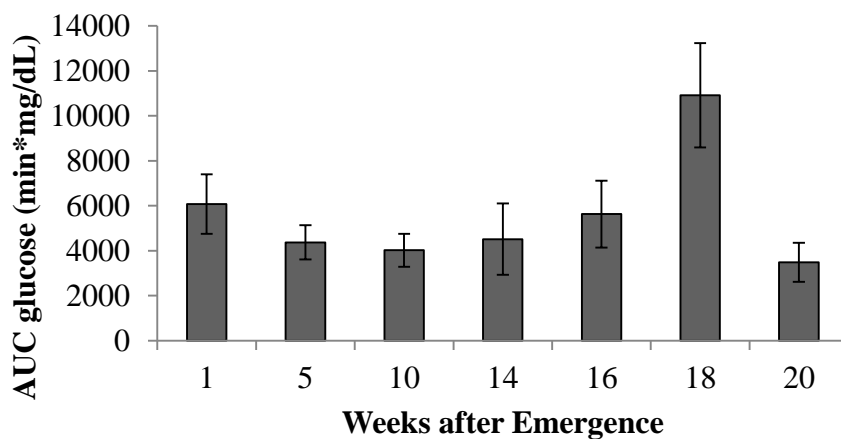


Figure 3.

Glucose intolerance was measured throughout the active season using IPGTT. A strong trend for an increase at 18 weeks post-emergence was found. Lines represent mean \pm SE of 6-9 squirrels for each week. $P = 0.077$.

Body temperature and visceral adipose mass do not vary significantly over the active season.

Body temperature did not vary over the active season, although there was a slight but non-significant drop at the last timepoint (Table 3). This is consistent with the observation that these squirrels were undergoing regular torpor bouts in the warm housing room. The masses of four visceral WAT depots as well as the sum of the depots (to give total visceral adipose mass) were analyzed. There was no change in the mass of any of the adipose depots nor in total visceral adipose mass over the active season, though it is important to note that the first tissue collection was 11 weeks after

emergence. Based on body mass, it is apparent that much of the increase in adipose mass had occurred prior to this time.

Table 3.
Body Temperature and Adipose Mass at Tissue Collection

Week Post-Emergence	11	15	17	19	21
T_b (°C)	37.5±1.1	37.2±0.5	37.0±0.3	36.9±1.4	36.0±1.8
iaWAT (g)	13.69±1.32	15.84±1.21	14.35±1.17	15.09±1.98	14.06±1.33
rWAT (g)	5.69±0.38	7.57±0.65	9.07±0.76	7.54±1.26	8.60±0.83
mWAT (g)	2.37±0.18	3.59±0.48	3.24±0.45	3.42±0.68	3.47±0.48
oWAT (g)	2.28±0.15	3.34±0.32	3.40±0.27	3.20±0.51	3.04±0.15
Total visceral WAT (g)	24.0±1.5	30.3±2.3	30.1±5.9	29.3±10.5	27.89±5.5
Adiposity (%)	10.0 ± 0.5	11.9 ± 0.4	11.9 ± 0.5	11.5 ± 1.1	11.4 ± 0.5

Body temperature (T_b) and masses of intra-abdominal (iaWAT), retroperitoneal (rWAT), mesenteric (mWAT) and omental (oWAT) depots were measured. Data represent means ± SE. P > 0.05 for all measurements.

Adipose tissue inflammatory state changes during the active season.

Obesity is often characterized by systemic, low-grade inflammation, particularly in adipose tissue. Cytokines and markers of certain immune populations were examined in WAT of 13-lined ground squirrels using RT-qPCR and ELISA. RT-qPCR was performed on iaWAT and mWAT using primers for immune cell markers to estimate immune cell populations (Table 1). In iaWAT, expression of FOXP3, a marker of Treg, was lower at week 11 than weeks 17 or 21 ($P = 0.012$; Figure 4A). MRC1, a marker of M2 macrophages, decreased between weeks 17 and 21 ($P = 0.05$; Figure 4B). Finally, there was a trend toward a progressive decrease in GATA3 throughout the active season ($P = 0.061$; Figure 4C). Both FOXP3 and MRC1 in iaWAT show a peak in expression at week 17. FOXP3 in mWAT shows no significant change in levels throughout the active season ($P = 0.096$; Figure 4D). In mWAT, MRC1 expression was lower at the very end of the active season compared to weeks 11 or 19 ($P = 0.007$; Figure 4E). mWAT GATA3 expression peaked 19 weeks after emergence ($P = 0.018$; Figure 4F).

Cytokine proteins were also measured in iaWAT (this work was performed in the lab by an undergraduate, Santidra Love) and ingWAT depots using ELISA. While concentrations of these cytokines in ingWAT (Figure 5D-F) did not change significantly over the active season, some displayed trends. Concentrations in visceral iaWAT (Figure 5A-C) changed in striking similarity to IPGTT results (Figure 3). In iaWAT, IL-10 levels were high early in the active season before dropping significantly 19 weeks after emergence ($P = 0.018$; Figure 5A). TNF α showed a different, and somewhat opposite trend, increasing progressively throughout the active season ($P = 0.001$; Figure 5B). IL-6

levels in drop significantly 19 weeks after emergence, but then increase rapidly to an all-season high at week 21 ($P = 0.002$; Figure 5C). In ingWAT, IL-10 displayed a trend toward decreasing throughout the active season, with the highest level occurring at week 11 ($P = 0.056$; Figure 5D). TNF α levels exhibited no change during the active season ($P = 0.2$; Figure 5E). IL-6 levels in ingWAT trended toward a peak 21 weeks after emergence ($P = 0.099$; Figure 5F).

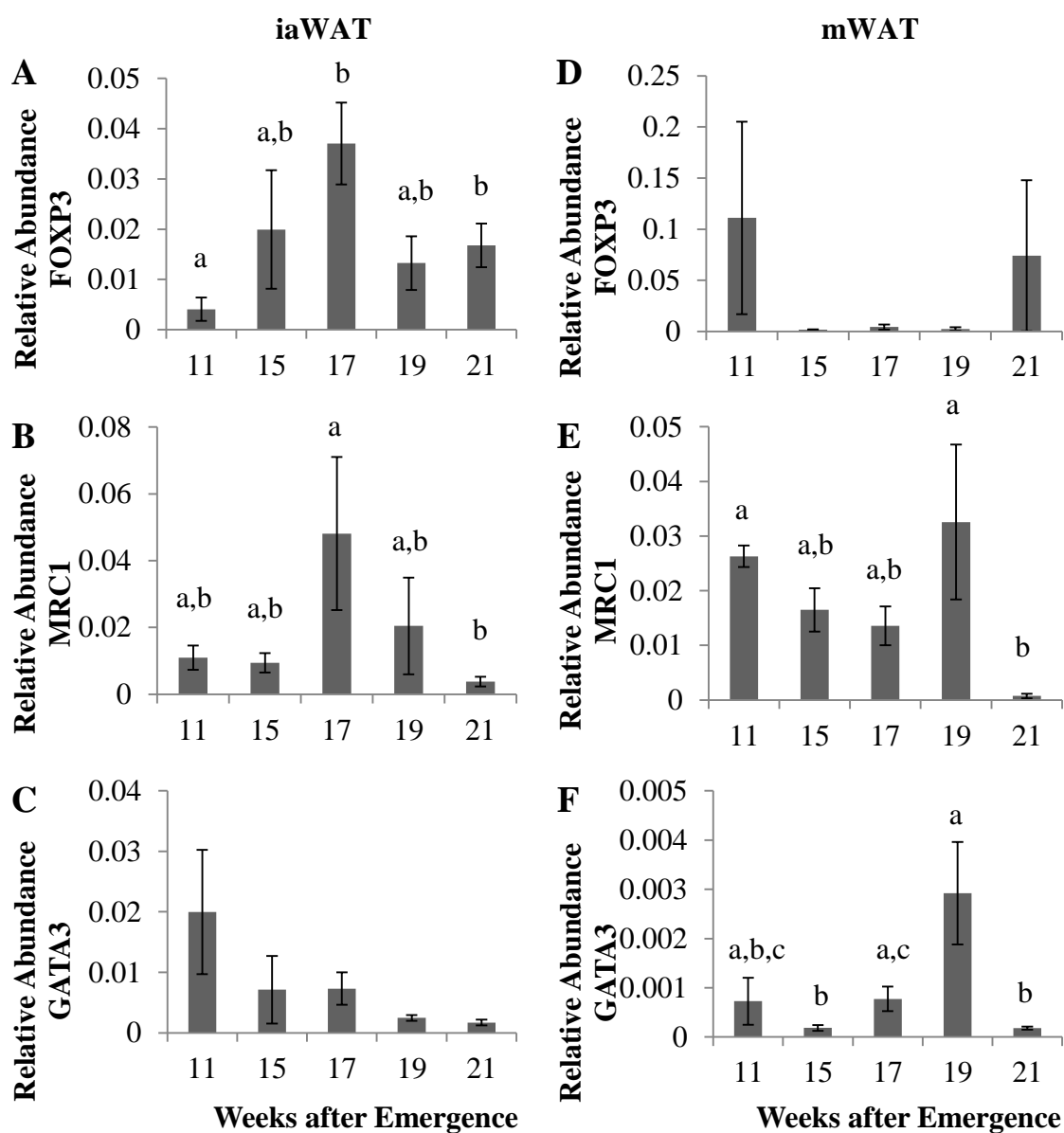


Figure 4.

Expression of immune cell markers in iaWAT (A-C) and mWAT (D-F) normalized to β -actin. (A) FOXP3 (Treg), ANOVA: $P < 0.05$. (B) MRC1 (M2 macrophages), ANOVA: $P = 0.05$. (C) GATA3 (Th2 cells), Kruskal-Wallis: $P > 0.05$. (D) FOXP3 (Treg), ANOVA: $P > 0.05$. (E) MRC1 (M2 macrophages), Kruskal-Wallis: $P < 0.05$. (F) GATA3 (Th2 cells), Kruskal-Wallis: $P < 0.05$.

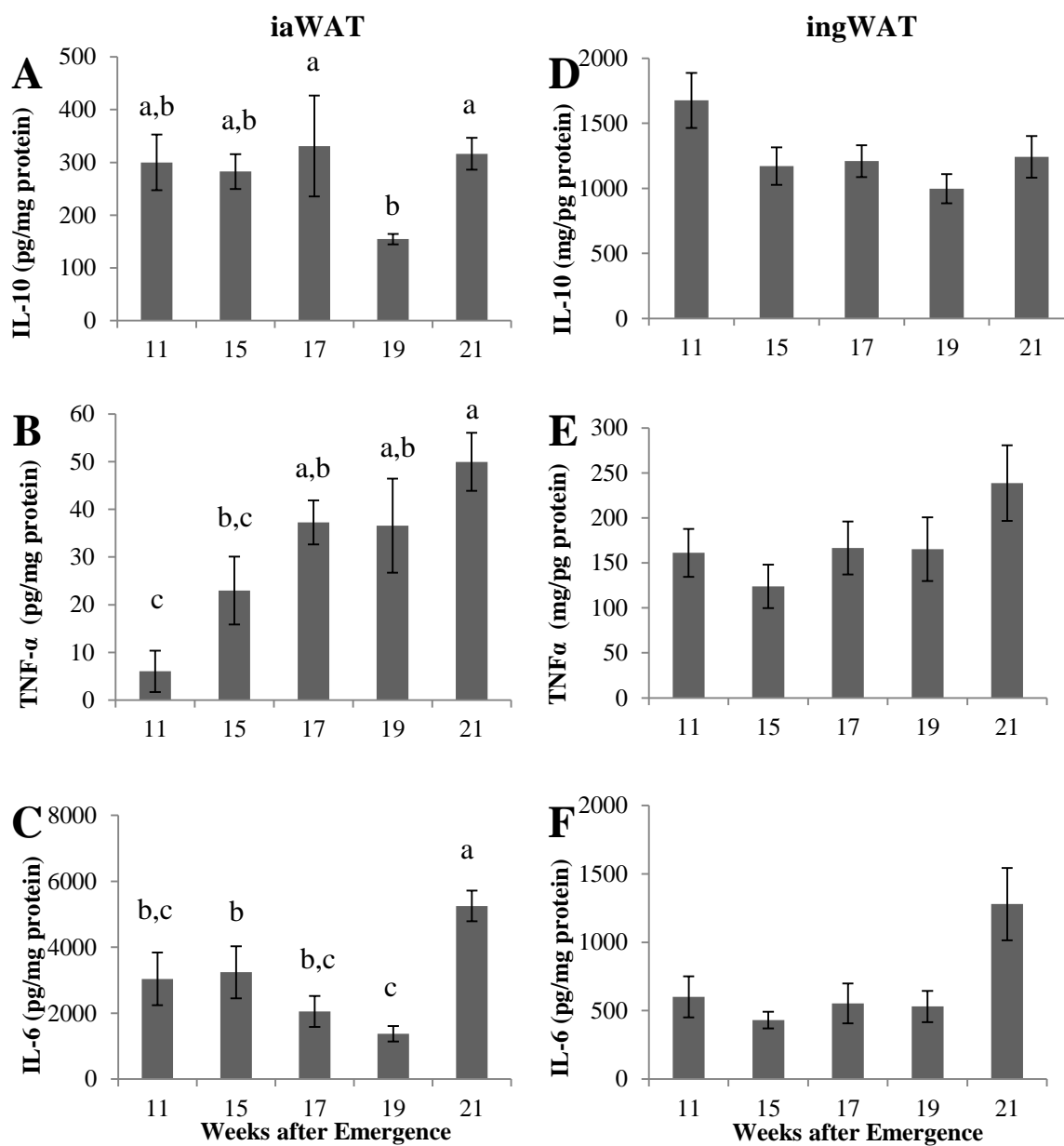


Figure 5.

Levels of IL-10 and TNF α in iaWAT (A-C) and ingWAT (D-F). (A) IL-10, ANOVA: $P < 0.05$. (B) TNF α , ANOVA: $P < 0.05$. (C) IL-6, ANOVA: $P > 0.05$. (D) IL-10, ANOVA: $P > 0.05$. (E) ingWAT TNF α , ANOVA: $P > 0.05$. (F) IL-6, ANOVA: $P < 0.05$.

Discussion

In this study, we examined changes in the physiology of 13-lined ground squirrels during their active season. As hibernators, 13-lined ground squirrels spend the majority of the year in torpor, during which time they are not consuming any nutrients and must rely solely on endogenous energy to survive. In the spring, these squirrels emerge from hibernation and must spend the next few months regaining the body weight and adiposity lost during hibernation and preparing for the subsequent hibernation season. In our study, we found that body mass increased and caloric intake peaked significantly during the active season, but adiposity did not change after mid-summer. Changes in the expression of important immune cell markers and cytokines in WAT point to a change in pro-inflammatory character, generally around 17-19 weeks after emergence. Though glucose tolerance did not change significantly during the active season, it did show a trend toward significant glucose intolerance around the same time.

Body mass increased steadily early in the active season, until it plateaued midway and stayed relatively constant for the remainder of the study. This suggests that by midway through the active season, optimal (or perhaps maximum) body mass had been achieved, which is consistent with the findings of other hibernator studies. In arctic ground squirrels, females have been found to achieve maximum body mass relatively early in the active season (within two months of emergence) compared to males, and then maintain that body mass through the remainder of the active season primarily through decreased metabolic rate (62). It is important to note the female ground squirrels were

also used for this study and, thus, studies of male ground squirrels are necessary to determine whether there is a sex difference in the increase in body mass in our species.

Unlike body mass, caloric intake peaked relatively early in the active season, which is consistent with other hibernators (54). Many hibernator species display a decrease in food intake following achievement of a threshold body mass, which is thought to be due to the increase in serum free fatty acid levels (54). In the wild, 13-lined ground squirrels will alter their diet during the active season to optimize weight and fat gain (51, 52, 54, 55). The diet shifts from herbivorous to granivorous, energy dense foods high in polyunsaturated fatty acids. High levels of polyunsaturated fatty acids can lower the melting point of the phospholipid membrane in preparation for the low body temperatures experienced during hibernation (51, 52). Though the contents of the diet in this study remained the same throughout the active season, previous studies have shown that hibernators are able to gain sufficient body mass and adiposity for hibernation even on a calorie-restricted diet (55). One study on chipmunks found that supplementing the diet with sunflower seed oil was sufficient to increase chipmunk hibernation bout duration relative to those fed a normal diet or one supplemented with saturated fatty acids (52). Furthermore, it has been found that many hibernators will not enter hibernation if not enough polyunsaturated fats are consumed for proper restructuring of phospholipid membranes (51). The small amount of sunflower seeds administered to the squirrels each week likely provided them with sufficient polyunsaturated fatty acids to hibernate. Indeed, many of the squirrels used in this study displayed short “test” bouts of torpor toward the end of the active season, which suggests that they had sufficient body mass,

adiposity, and polyunsaturated fatty acid consumption despite the inability to select different diets.

One mechanism for continued increase in body mass despite a decrease in caloric intake is a decrease in metabolic rate. Many species of hibernators have been found to display decreases in metabolic rate and body temperature prior to the onset of obesity (51, 52). In addition, 13-lined ground squirrels and other hibernators exhibit short “test” bouts of torpor in preparation for hibernation, which can last less than a day up to multiple days (51, 63). These bouts of torpor occur independently of cold exposure, and are entrained to a circannual rhythm. In our study, by the end of the active season, some squirrels displayed these “test” bouts. During these bouts, the animals felt cold and could not be easily aroused by noise or activity. By allowing their metabolic rate and body temperature to fall during these short bouts of torpor, the squirrels were able to maintain a relatively constant body mass despite decreased caloric intake.

The gut microbiota of hibernators changes markedly throughout the year, with the influx of dietary substrates at the beginning of the active season shifting the gut microbiota of hibernators to more *Firmicutes* and less *Bacteroidetes* and *Verrucomicrobia* (53, 55, 59). *Firmicutes* prefer dietary substrates, particularly carbohydrates; the influx of which leads to increased *Firmicutes* during the active season (53, 59). On the other hand, *Bacteroidetes* are able to use either dietary or host-derived substrates and *Verrucomicrobia* specializes in utilizing host-derived substrates, making both groups less dominant in the substrate-rich environment of the active season gut (53, 59). The shift from *Bacteroidetes* to *Firmicutes* results in an overall shift of the active

season gut microbiota toward a composition that promotes fattening through more efficient energy harvest and signals to the host to enhance storage of energy in adipose tissue (55, 60). This likely contributed to the continued increase in body mass even after the caloric intake decreased; the animals would simply be able to absorb more nutrients from the food that they consume, thanks to a more efficient gut microbiota.

Visceral adipose mass showed no change in the squirrels euthanized between 11 and 21 weeks after emergence. Presumably, the majority of visceral adipose mass was already acquired by this point, as is suggested by the levelling off of body mass that began around ten weeks post-emergence. Fat mass gain in hibernators is achieved to a certain “preferred” level, so it is possible that the squirrels used in this study had already achieved the necessary threshold of fat mass by week 11, so they did not acquire much fat mass beyond that point (52). This is in stark contrast to the pattern of adipose mass gain in other hibernators, which have been found to gain the majority of their fat mass late in the active season (52).

Insulin resistance (IR) is commonly associated with obesity. Though we did not measure insulin levels or physiological response to insulin directly in this study, the glucose tolerance of the squirrels was analyzed throughout the active season to act as a proxy for insulin sensitivity. During normal insulin function, when food is ingested, insulin is secreted from the pancreas and travels in the bloodstream to other tissues (such as muscle) where it induces the translocation of GLUT4 into the cell membrane (4, 6, 7). This allows for cellular uptake of glucose from the bloodstream, which causes blood glucose levels to drop. During IR, insulin is unable to induce the integration of GLUT4

into the cellular membrane, leading to increased levels of glucose in the blood after feeding (4). Previous studies with other hibernators have shown that they develop IR late in the active season, but that insulin sensitivity is recovered just before the animals enter hibernation, possibly due to antioxidant production (51, 54). As such, we expected our results to show a similar trend, with IR (measured as glucose intolerance) reaching a peak late in the active season, but decreasing just before hibernation should begin. Though no significant change was detected, there was a trend toward a significant peak in glucose intolerance 18 weeks after emergence. This suggests that IR had developed at this time, but insulin sensitivity and glucose tolerance are quickly recovered by week 20, which is consistent with previous studies on hibernators.

Interestingly, around the same time that glucose tolerance was at its lowest, there were significant changes occurring in the immune state of the visceral adipose tissue. IR has been long thought to be the result of adipose tissue inflammation (40, 42, 43, 48), but a recent paper suggests the opposite may be true and that IR may contribute to the development of adipose inflammation (48). Regardless of the direction of effect, both IR and adipose tissue inflammation commonly occur together during obesity. In obesity, adipose tissue typically displays increases in pro-inflammatory immune cell populations and decreases in anti-inflammatory immune cell populations, resulting in an overall increase in inflammatory state (40–42, 44, 45, 47, 57, 64, 65). Though it is commonly accepted that adipose tissue inflammation contributes to the development of obesity, obesity also contributes to changes in adipose immune state through differential secretion of adipokines (5, 47). Anti-inflammatory cells in particular are influenced by obese

adipokine levels, which create an unfavorable environment for their survival and proliferation. Adiponectin has a positive effect on both Treg cell proliferation and M2 macrophage IL-10 production, but is decreased in obesity (47). On the other hand, leptin levels are increased in obesity, leading to decreased Treg cell proliferation (47). In general, the populations of anti-inflammatory immune cells peak around 17-19 weeks after emergence, then drop to similar levels that they were at prior to the peak. The reason for the increase in anti-inflammatory immune cells at this time, when IR has presumably developed and adipose inflammation is high, is likely compensatory. Due to the increasing levels of adipose inflammation, the levels of Tregs, M2 macrophages, and Th2 cells likely increase to try to offset this inflammation, but decrease again once the inflammatory state progressed to a point where it caused an unsuitable environment for these anti-inflammatory cells to survive and proliferate. Though there are few studies on the immune changes that occur in hibernators during the active season (most focus on differences between active and hibernating animals) and no studies on WAT immune cells in hibernators, there has been some evidence for immune suppression in other tissues occurring in autumn in preparation for hibernation (66, 67). In particular, small lymphocytes and B cells in lymph nodes decrease in number in autumn, along with the cytotoxic activity of T cells, but populations of splenic T cells and peritoneal macrophages have been found to increase (67). However, without evidence from the adipose tissue of other hibernator species, the difference may be simply attributed to differences between the tissues or species studied. Overall, the anti-inflammatory

immune cell populations in our squirrels showed a slightly different pattern than seen in obesity in other models.

Though immune cell populations can give an idea of the immune state of adipose tissue, the better indicator is the levels of pro-inflammatory and anti-inflammatory cytokines, because cytokines are the actual modulators of immune function. Significant changes in TNF- α , IL-10, and IL-6 in iaWAT but not ingWAT support previous evidence that suggests visceral adipose tissue inflammation, but not subcutaneous inflammation, corresponds with obesity (40, 42, 68). The cytokines analyzed in this study, TNF α and IL-10, represent the primary pro-inflammatory and anti-inflammatory cytokines, respectively. IL-6 also has primarily pro-inflammatory properties in obese adipose tissue (69). TNF α is a pro-inflammatory cytokine that is produced by M1 (“classically activated”; pro-inflammatory) macrophages, Th1 cells, dendritic cells, and mast cells which has been found to be increased in WAT during obesity (40–42, 44, 45, 47, 65, 68). TNF α has been linked to the development of IR, which is supported by the timing of the peaks in TNF α and glucose intolerance that we saw in this study (70). On the other hand, IL-10 is an anti-inflammatory cytokine primarily produced by M2 (“alternately activated”; anti-inflammatory) macrophages as well as Treg and Th2 cells (40, 42, 47, 71). IL-10 has been associated with protection against TNF α -dependent IR (42). We found that IL-10 drops dramatically 19 weeks after emergence; at the same time or just after the levels of M2 macrophages, Tregs, and Th2 cells increase. This discrepancy may be due to a decreased activity of the anti-inflammatory immune cells, resulting in an increase in population but no apparent decrease in adipose inflammation.

IL-6 has also been found to contribute to IR during obesity (69). IL-6 is produced primarily by mast cells, M1 macrophages, and Th1 cells, and its production is inhibited by IL-10 (71, 72). This interaction between IL-6 and IL-10 support our data, which show a rapid increase in IL-6 immediately following the lowest levels of IL-10 of the active season.

Overall, our results point to a peak in caloric intake occurring prior to maximum body mass being achieved and significant changes in the adipose immune state and glucose tolerance of the squirrels between 17 and 19 weeks after emergence, but no changes in visceral adipose mass. We propose that the drastic changes in visceral adipose mass found in other studies of hibernators would have been observed here if our first tissue collection occurred at the beginning of the active season. Our results suggest that these squirrels follow the same relative progression of obesity as in other animal models and humans and, as such, may be used to determine possible therapeutic treatments for obesity. Due to the ability of ground squirrels, and other hibernators, to gain sufficient weight for hibernation despite a calorie-restricted diet (55), it is evident that they are programmed to gain excess amounts of body mass and adiposity over the short active season. If there is a way to inhibit hibernators from becoming obese, even when they have such a strong genetic predisposition toward it, then it is likely that similar treatments could work on non-hibernating species.

Chapter III

Conclusion

Hibernators, such as the 13-lined ground squirrel (*Ictidomys tridecemlineatus*), spend a significant portion of the year hibernating, which is characterized by the reliance on endogenous energy stores for survival (51, 53–55, 58, 59). Due to this extended period of voluntary fasting, 13-lined ground squirrels need to build up large fat stores in their bodies prior to entering hibernation, which is accomplished during their short, 4-5 month active season (51, 53–55). Toward the end of the active season, the squirrels develop obesity and IR.

We monitored various aspects of 13-lined ground squirrel physiology during the active season to determine changes in body mass, caloric intake, adiposity, glucose tolerance, and adipose tissue inflammation that occurred during the development of obesity. We examined changes in body mass and caloric intake over the active season. Like other hibernators, the squirrels underwent a hyperphagic period, but the caloric intake dropped off prior to the squirrels reaching their maximum body mass (51, 53–55). Given the shift in the gut microbiota of obese mammals to a more energy-efficient state, we suspect that the gut microbiota shifted around the same time as the peak caloric intake, resulting in continued mass gain despite decreased caloric intake (24, 26). Surprisingly, we did not detect any changes in visceral adipose mass or adiposity during the weeks that tissue collections were performed. Though previous studies on hibernators suggest that the majority of adipose mass is gained late in the active season, we speculate

that our squirrels actually gained large amounts of adipose mass at the beginning of the active season, resulting in very little change after the midpoint (55). Late in the active season, our squirrels displayed a change in adipose immune state and a corresponding trend toward IR, which is consistent with the findings of previous research that adipose inflammation and IR are closely tied together (40, 41, 45, 47, 48).

We propose that by performing the first tissue collection at the beginning of the active season, future studies may be able to detect certain changes that were not found to be significant in our study, such as changes in adiposity. In addition, analyzing the composition of the gut microbiota and intestinal immune state during the active season may elucidate certain mechanisms of weight gain and obesity pathogenesis that have been seen in other models. Additionally, understanding the interaction of the gut microbiota and adipose inflammation with the development of obesity through the administration of antibiotics, probiotics or anti-inflammatory drugs could allow a better understanding of the causal relationships during obesity development. Finally, additional research on the development of obesity in 13-lined ground squirrels during the active season could be beneficial in determining pharmaceutical treatments for obesity in other animal models and potentially humans.

References

1. Morris MJ, Beilharz JE, Maniam J, Reichelt AC, Westbrook RF. 2015. Why is obesity such a problem in the 21st century? The intersection of palatable food, cues and reward pathways, stress, and cognition. *Neurosci Biobehav Rev* 58:36–45.
2. Klok MD, Jakobsdottir S, Drent ML. 2007. The role of leptin and ghrelin in the regulation of food intake and body weight in humans: a review. *Obes Rev* 8:21–34.
3. Morton GJ, Cummings DE, Baskin DG, Barsh GS, Schwartz MW. 2006. Central nervous system control of food intake and body weight. *Nature* 443:289–295.
4. Pereira-Lancha LO, Coelho DF, de Campos-Ferraz PL, Lancha Jr AH. 2010. Body fat regulation: is it a result of a simple energy balance or a high fat intake? *J Am Coll Nutr* 29:343–351.
5. Lago R, Gómez R, Lago F, Gómez-Reino J, Gualillo O. 2008. Leptin beyond body weight regulation—Current concepts concerning its role in immune function and inflammation. *Cell Immunol* 252:139–145.
6. Nonogaki K. 2000. New insights into sympathetic regulation of glucose and fat metabolism. *Diabetologia* 43:533–549.
7. Greenway SC. 2004. Hormones in Human Metabolism and Disease, p. 271–294. *In* Storey, KB (ed.), *Functional metabolism: regulation and adaptation*. John Wiley & Sons, Hoboken, N.J.

8. la Fleur SE, Luijendijk MCM, van der Zwaal EM, Brans MAD, Adan RAH. 2014. The snacking rat as model of human obesity: effects of a free-choice high-fat high-sugar diet on meal patterns. *Int J Obes* 38:643–649.
9. O'Rourke RW. 2014. Metabolic Thrift and the Genetic Basis of Human Obesity: *Ann Surg* 259:642–648.
10. Speakman J, Hambly C, Mitchell S, Krol E. 2008. The contribution of animal models to the study of obesity. *Lab Anim* 42:413–432.
11. Nilsson C, Raun K, Yan F, Larsen MO, Tang-Christensen M. 2012. Laboratory animals as surrogate models of human obesity. *Acta Pharmacol Sin* 33:173–181.
12. Kanasaki K, Koya D. 2011. Biology of Obesity: Lessons from Animal Models of Obesity. *J Biomed Biotechnol* 2011:1–11.
13. Spurlock ME, Gabler NK. 2008. The development of porcine models of obesity and the metabolic syndrome. *J Nutr* 138:397–402.
14. 2017. Obesity and Overweight. World Health Organ.
15. Bastard J-P, Maachi M, Lagathu C, Kim MJ, Caron M, Vidal H, Capeau J, Fève B. 2006. Recent advances in the relationship between obesity, inflammation, and insulin resistance. *Eur Cytokine Netw* 17:4–12.

16. Bischoff SC, Barbara G, Buurman W, Ockhuizen T, Schulzke J-D, Serino M, Tilg H, Watson A, Wells JM. 2014. Intestinal permeability—a new target for disease prevention and therapy. *BMC Gastroenterol* 14:189.
17. Garidou L, Pomié C, Klopp P, Waget A, Charpentier J, Aloulou M, Giry A, Serino M, Stenman L, Lahtinen S, Dray C, Iacovoni JS, Courtney M, Collet X, Amar J, Servant F, Lelouvier B, Valet P, Eberl G, Fazilleau N, Douin-Echinard V, Heymes C, Burcelin R. 2015. The Gut Microbiota Regulates Intestinal CD4 T Cells Expressing ROR γ t and Controls Metabolic Disease. *Cell Metab* 22:100–112.
18. Gulhane M, Murray L, Lourie R, Tong H, Sheng YH, Wang R, Kang A, Schreiber V, Wong KY, Magor G, Denman S, Begun J, Florin TH, Perkins A, Cuív PÓ, McGuckin MA, Hasnain SZ. 2016. High Fat Diets Induce Colonic Epithelial Cell Stress and Inflammation that is Reversed by IL-22. *Sci Rep* 6.
19. Kim K-A, Gu W, Lee I-A, Joh E-H, Kim D-H. 2012. High Fat Diet-Induced Gut Microbiota Exacerbates Inflammation and Obesity in Mice via the TLR4 Signaling Pathway. *PLoS ONE* 7:e47713.
20. Konrad D, Wueest S. 2014. The Gut-Adipose-Liver Axis in the Metabolic Syndrome. *Physiology* 29:304–313.
21. Ley RE, Bäckhed F, Turnbaugh P, Lozupone CA, Knight RD, Gordon JI. 2005. Obesity alters gut microbial ecology. *Proc Natl Acad Sci U S A* 102:11070–11075.

22. Saad MJA, Santos A, Prada PO. 2016. Linking Gut Microbiota and Inflammation to Obesity and Insulin Resistance. *Physiology* 31:283–293.
23. Winer D, Luck H, Tsai S, Winer S. 2016. The Intestinal Immune System in Obesity and Insulin Resistance. *Cell Metab* 23:413–426.
24. Burcelin R, Serino M, Chabo C, Garidou L, Pomié C, Courtney M, Amar J, Bouloumié A. 2013. Metagenome and metabolism: the tissue microbiota hypothesis. *Diabetes Obes Metab* 15:61–70.
25. McPhee JB, Schertzer JD. 2015. Immunometabolism of obesity and diabetes: microbiota link compartmentalized immunity in the gut to metabolic tissue inflammation. *Clin Sci* 129:1083–1096.
26. Schroeder BO, Bäckhed F. 2016. Signals from the gut microbiota to distant organs in physiology and disease. *Nat Med* 22:1079–1089.
27. Sonnenburg JL, Bäckhed F. 2016. Diet–microbiota interactions as moderators of human metabolism. *Nature* 535:56–64.
28. Lee SH. 2015. Intestinal Permeability Regulation by Tight Junction: Implication on Inflammatory Bowel Diseases. *Intest Res* 13:11.
29. McKay DM, Baird AW. 1999. Cytokine regulation of epithelial permeability and ion transport. *Gut* 44:283–289.

30. Ménard S, Cerf-Bensussan N, Heyman M. 2010. Multiple facets of intestinal permeability and epithelial handling of dietary antigens. *Mucosal Immunol* 3:247–259.
31. Ding S, Lund PK. 2011. Role of intestinal inflammation as an early event in obesity and insulin resistance: *Curr Opin Clin Nutr Metab Care* 14:328–333.
32. Moritz Leppkes, Manolis Roulis, Markus F. Neurath, George Kollias, Christoph Becker. 2014. Pleiotropic functions of TNF- α in the regulation of the intestinal epithelial response to inflammation.pdf. *Jpn Soc Immunol* 26:509–515.
33. Sartor RB. 1994. Cytokines in intestinal inflammation: pathophysiological and clinical considerations. *Gastroenterology* 106:533–539.
34. Waldner MJ, Neurath MF. 2014. Master regulator of intestinal disease: IL-6 in chronic inflammation and cancer development. *Semin Immunol* 26:75–79.
35. Monteiro-Sepulveda M, Touch S, Mendes-Sá C, André S, Poitou C, Allatif O, Cotillard A, Fohrer-Ting H, Hubert E-L, Remark R, Genser L, Tordjman J, Garbin K, Osinski C, Sautès-Fridman C, Leturque A, Clément K, Brot-Laroche E. 2015. Jejunal T Cell Inflammation in Human Obesity Correlates with Decreased Enterocyte Insulin Signaling. *Cell Metab* 22:113–124.
36. Hue S, Ahern P, Buonocore S, Kullberg MC, Cua DJ, McKenzie BS, Powrie F, Maloy KJ. 2006. Interleukin-23 drives innate and T cell-mediated intestinal inflammation. *J Exp Med* 203:2473–2483.

37. Schreiber F, Arasteh JM, Lawley TD. 2015. Pathogen Resistance Mediated by IL-22 Signaling at the Epithelial–Microbiota Interface. *J Mol Biol* 427:3676–3682.
38. Asseman C, Mauze S, Leach MW, Coffman RL, Powrie F. 1999. An essential role for interleukin 10 in the function of regulatory T cells that inhibit intestinal inflammation. *J Exp Med* 190:995–1004.
39. Lee JS, Tato CM, Joyce-Shaikh B, Gulen MF, Cayatte C, Chen Y, Blumenschein WM, Judo M, Ayanoglu G, McClanahan TK, Li X, Cua DJ. 2015. Interleukin-23-Independent IL-17 Production Regulates Intestinal Epithelial Permeability. *Immunity* 43:727–738.
40. Boutens L, Stienstra R. 2016. Adipose tissue macrophages: going off track during obesity. *Diabetologia* 59:879–894.
41. Lago F, Dieguez C, Gomezreino J, Gualillo O. 2007. The emerging role of adipokines as mediators of inflammation and immune responses. *Cytokine Growth Factor Rev* 18:313–325.
42. Lumeng CN, Bodzin JL, Saltiel AR. 2007. Obesity induces a phenotypic switch in adipose tissue macrophage polarization. *J Clin Invest* 117:175–184.
43. Sun S, Ji Y, Kersten S, Qi L. 2012. Mechanisms of Inflammatory Responses in Obese Adipose Tissue. *Annu Rev Nutr* 32:261–286.

44. Weisberg SP, McCann D, Desai M, Rosenbaum M, Leibel RL, Ferrante AW. 2003. Obesity is associated with macrophage accumulation in adipose tissue. *J Clin Invest* 112:1796–1808.
45. Kintscher U, Hartge M, Hess K, Foryst-Ludwig A, Clemenz M, Wabitsch M, Fischer-Posovszky P, Barth TFE, Dragun D, Skurk T, Hauner H, Bluher M, Unger T, Wolf A-M, Knippschild U, Hombach V, Marx N. 2008. T-lymphocyte Infiltration in Visceral Adipose Tissue: A Primary Event in Adipose Tissue Inflammation and the Development of Obesity-Mediated Insulin Resistance. *Arterioscler Thromb Vasc Biol* 28:1304–1310.
46. Ferrante AW. 2013. The immune cells in adipose tissue. *Diabetes Obes Metab* 15:34–38.
47. Feuerer M, Herrero L, Cipolletta D, Naaz A, Wong J, Nayer A, Lee J, Goldfine AB, Benoist C, Shoelson S, Mathis D. 2009. Lean, but not obese, fat is enriched for a unique population of regulatory T cells that affect metabolic parameters. *Nat Med* 15:930–939.
48. Shimobayashi M, Albert V, Woelnerhanssen B, Frei IC, Weissenberger D, Meyer-Gerspach AC, Clement N, Moes S, Colombi M, Meier JA, Swierczynska MM, Jenö P, Beglinger C, Peterli R, Hall MN. 2018. Insulin resistance causes inflammation in adipose tissue. *J Clin Invest* 128:1538–1550.

49. Burcelin R, Serino M, Chabo C, Blasco-Baque V, Amar J. 2011. Gut microbiota and diabetes: from pathogenesis to therapeutic perspective. *Acta Diabetol* 48:257–273.
50. Lutz TA, Woods SC. 2012. Overview of Animal Models of Obesity, p. . *In* Enna, SJ, Williams, M, Barret, JF, Ferkany, JW, Kenakin, T, Porsolt, RD (eds.), *Current Protocols in Pharmacology*. John Wiley & Sons, Inc., Hoboken, NJ, USA.
51. Storey KB, Storey JM. 2004. Mammalian Hibernation: Biochemical Adaptation and Gene Expression, p. 443–471. *In* Storey, KB (ed.), *Functional metabolism: regulation and adaptation*. John Wiley & Sons, Hoboken, N.J.
52. Dark J. 2005. ANNUAL LIPID CYCLES IN HIBERNATORS: Integration of Physiology and Behavior. *Annu Rev Nutr* 25:469–497.
53. Carey HV, Walters WA, Knight R. 2013. Seasonal restructuring of the ground squirrel gut microbiota over the annual hibernation cycle. *Am J Physiol-Regul Integr Comp Physiol* 304:R33–R42.
54. Florant GL, Healy JE. 2012. The regulation of food intake in mammalian hibernators: a review. *J Comp Physiol B* 182:451–467.
55. Hatton JJ, Stevenson TJ, Buck CL, Duddleston KN. 2017. Diet affects arctic ground squirrel gut microbial metatranscriptome independent of community structure: Microbiota of fattening arctic ground squirrels. *Environ Microbiol* 19:1518–1535.

56. Sheriff MJ, Fridinger RW, Tøien øivind, Barnes BM, Buck CL. 2013. Metabolic Rate and Prehibernation Fattening in Free-Living Arctic Ground Squirrels. *Physiol Biochem Zool* 86:515–527.
57. Cavallari JF, Denou E, Foley KP, Khan WI, Schertzer JD. 2016. Different Th17 immunity in gut, liver, and adipose tissues during obesity: the role of diet, genetics, and microbes. *Gut Microbes* 7:82–89.
58. Carey HV, Pike AC, Weber CR, Turner JR, Visser A, Beijer-Liefers SC, Bouma HR, Kroese FGM. 2012. Impact of Hibernation on Gut Microbiota and Intestinal Barrier Function in Ground Squirrels, p. 281–291. *In* Ruf, T, Bieber, C, Arnold, W, Millesi, E (eds.), *Living in a Seasonal World*. Springer Berlin Heidelberg, Berlin, Heidelberg.
59. Stevenson TJ, Duddleston KN, Buck CL. 2014. Effects of Season and Host Physiological State on the Diversity, Density, and Activity of the Arctic Ground Squirrel Cecal Microbiota. *Appl Environ Microbiol* 80:5611–5622.
60. Stevenson TJ, Buck CL, Duddleston KN. 2014. Temporal Dynamics of the Cecal Gut Microbiota of Juvenile Arctic Ground Squirrels: a Strong Litter Effect across the First Active Season. *Appl Environ Microbiol* 80:4260–4268.
61. Leopoldo AS, Lima-Leopoldo AP, Nascimento AF, Luvizotto RAM, Sugizaki MM, Campos DHS, da Silva DCT, Padovani CR, Cicogna AC. 2016. Classification of different degrees of adiposity in sedentary rats. *Braz J Med Biol Res* 49.

62. Buck CL, Barnes BM. 1999. Annual cycle of body composition and hibernation in free-living arctic ground squirrels. *J Mammal* 80:430–442.
63. Russell RL, O'Neill PH, Epperson LE, Martin SL. 2010. Extensive use of torpor in 13-lined ground squirrels in the fall prior to cold exposure. *J Comp Physiol B* 180:1165–1172.
64. Strissel KJ, DeFuria J, Shaul ME, Bennett G, Greenberg AS, Obin MS. 2010. T-Cell Recruitment and Th1 Polarization in Adipose Tissue During Diet-Induced Obesity in C57BL/6 Mice. *Obesity* 18:1918–1925.
65. Zuniga LA, Shen W-J, Joyce-Shaikh B, Pyatnova EA, Richards AG, Thom C, Andrade SM, Cua DJ, Kraemer FB, Butcher EC. 2010. IL-17 Regulates Adipogenesis, Glucose Homeostasis, and Obesity. *J Immunol* 185:6947–6959.
66. Shivatcheva TM. 1989. Circannual variations of the immune system of hibernators, p. 87–95. *In Living in the Cold*. John Libbey Eurotext, Paris.
67. Novoselova EG, Kolaeva SG, Makar VR, Agaphonova TA. 2000. Production of tumor necrosis factor in cells of hibernating ground squirrels *Citellus undulatus* during annual cycle. *Life Sci* 67:1073–1080.
68. Altintas MM, Azad A, Nayer B, Contreras G, Zaias J, Faul C, Reiser J, Nayer A. 2011. Mast cells, macrophages, and crown-like structures distinguish subcutaneous from visceral fat in mice. *J Lipid Res* 52:480–488.

69. Xu H. 2013. Obesity and metabolic inflammation. *Drug Discov Today Dis Mech* 10:e21–e25.
70. Moller DE. 2000. Potential role of TNF- α in the pathogenesis of insulin resistance and type 2 diabetes. *Trends Endocrinol Metab* 11:212–217.
71. Couper KN, Blount DG, Riley EM. 2008. IL-10: The Master Regulator of Immunity to Infection. *J Immunol* 180:5771–5777.
72. Becker M, Levings MK, Daniel C. 2017. Adipose-tissue regulatory T cells: Critical players in adipose-immune crosstalk. *Eur J Immunol* 47:1867–1874.